ELSEVIER

Journal of Nuclear Materials 264 (1999) 169–179

journal of nuclear materials

Mössbauer spectroscopy of tin in unirradiated and neutron irradiated Zircaloys

Jerzy A. Sawicki *

AECL, Chalk River Laboratories, Chalk River, Ont., Canada KOJ 1JO

Received 24 March 1998; accepted 17 June 1998

Abstract

Mössbauer spectroscopy of the 23.9 keV γ-rays in ^{119}Sn nuclei was applied to study Zircaloy-2, Zircaloy-4, and other tin-bearing zirconium-based alloys of interest to nuclear power technology. Zircaloys are extensively used in nuclear reactors as fuel cladding. In CANDU reactors, Zircaloys are also used as major structural components such as calandria tubes, and were used until the late 1970's as pressure tubes (now replaced by Zr–2.5Nb alloy). Unirradiated specimens of these alloys, as well as radioactive specimens, both neutron-irradiated in high-flux test reactors and extracted from nuclear power-reactor components after many years of service, were examined. The obtained spectra consistently showed tin in substitutional solid solution in α-Zr, whereas no evidence was found of metallic Sn or intermetallic Zr_4Sn precipitates. In oxide scrapes removed from Zircaloy-2 pressure tube of one of CANDU reactors, where the alloy was exposed for about 10 years to pressurized heavy water coolant at temperatures of ~280°C, a considerable fraction of tin was found in the Sn(IV) state, in the form that coincides with the state of tin in stannic oxide, SnO_2. The same form of tin was identified in filterable deposits in the primary heavy water coolant of CANDU reactors. For comparison, in Zircaloy heated in air, SnO_2 was formed only at temperatures above 500°C.

1. Introduction

Zirconium-based alloys, Zircaloy-2 (approx. Zr–1.5 Sn–0.15Fe–0.1Cr–0.05Ni% [1]) and Zircaloy-4 (approx. Zr–1.5Sn–0.25Fe–0.1Cr%), are used widely as fuel cladding and core structural material in light- and heavy-water cooled nuclear reactors. In particular, in pressurized heavy-water cooled reactors of CANDU [2] type, Zircaloy-2 is being used as the calandria tubes, whereas Zircaloy-4 is used as fuel sheathing, and had been also used in earlier CANDU plants as pressure tubes (now replaced by tin-free Zr–2.5%Nb alloy).

Zircaloys are essentially single-phase α-Zr stabilized by Sn in supersaturated solid solution. The Fe, Cr and Ni are virtually insoluble in α-Zr and thus occur in these alloys as intermetallic precipitates of $Zr(Fe,Cr)_2$ and $Zr_2(Fe,Ni)$. The presence of these precipitates strongly affects the corrosion, hydriding and fracture properties of Zircaloys in the nuclear reactors. The structure and composition of the precipitates change considerably during irradiation at power reactor temperatures (~300°C). In particular, it has been found that the precipitates become amorphous upon irradiation and the transition elements preferentially diffuse out of the intermetallic particles [1,2]. The precipitates in Zircaloys have been extensively studied using analytical electron-microscopy, whereas other microscopic methods, and especially the hyperfine-interaction techniques have not until recently been employed in theses studies.

First applications of ^{57}Fe Mössbauer spectroscopy in studies of iron-bearing intermetallic precipitates in Zircaloys were reported by us recently [3,4]. The purpose of the present investigation was to assess the use of

* Corresponding author. Tel.: +1-613 584 8811; fax: +1-613 584 1220; e-mail: sawicki@acel.ca.

[1] Throughout the text, the alloy compositions are given in wt%.

[2] CANDU^R is a registered trademark of Atomic Energy of Canada Limited (AECL).

0022-3115/99/$ – see front matter
PII: S0022-3115(98)00463-2

Mössbauer spectra of ^{119}Sn in studying the state of tin in unirradiated, irradiated and oxidized commercial Zircaloy-2 and -4. The study was performed to get information on the behavior of tin in Zircaloys, and especially in reactor-irradiated specimens. Although, according to the binary Zr–Sn phase diagram [5], Sn should remain in solid solution with α-Zr, metallic Sn precipitates and various Sn-rich intermetallic precipitates were reported in several electron microscopic observations, particularly after high-temperature oxidation and irradiation of Zircaloys [6–12]. Further, the behavior of tin and its role in oxidation of Zircaloys in water and steam at power reactor conditions remains to be fully explained. The high-temperature chemistry of tin in irradiated Zircaloy fuel cladding is also of interest.

2. Experimental technique

The resonant 23.9 keV M1-transition in ^{119}Sn between spin states $1/2^+$ (ground state) and $3/2^+$ (first excited state, $T_{1/2} = 17.8$ ns) ranks second in usefulness (after the 14.4 keV ^{57}Fe resonance) in Mössbauer spectroscopy [13]. The 23.9 keV transition is populated by the isomeric transition from metastable ^{119m}Sn ($E_\gamma = 65.7$ keV, $T_{1/2} = 293$ d), which can be prepared by neutron capture in isotopically enriched ^{118}Sn. Measurements of the Mössbauer spectra of tin are facilitated by the rather high natural isotopic content of ^{119}Sn (8.6%), the high resonant absorption cross section for 23.9 keV γ-rays ($\sigma_0 = 1.4 \times 10^{-22}$ m^2), low recoil energy ($E_r = 2.6 \times 10^{-3}$ eV) and the small natural width of the absorption line ($2\Gamma = 0.65$ mm/s).

The measurements were performed using a 5 mCi (185 MBq) source of ^{119m}Sn in $CaSnO_3$ matrix. The source had an active diameter of 13 mm, a recoilless fraction, f_S, of about 0.5, and a source line-width, Γ_A, of less than 0.4 mm/s. The γ-rays were detected using an intrinsic planar Ge detector capable of resolving the 23.9 keV Mössbauer γ-rays from the 25.0 keV and 25.3 keV K_α Sn X-rays, the latter resulting from the 65.7 keV γ-ray, which is strongly internally converted. Typical γ-ray emission spectra for the $CaSnO_3$ source and neutron-irradiated (radioactive) Zircaloy specimen are compared in Fig. 1(a) and (b), respectively. As seen, the Mössbauer γ-rays could be well separated from all interfering lines in the spectrum.

During all measurements the source and absorbers were kept at 295 K. The velocity scale of the Mössbauer spectra was calibrated with respect to a standard 25 μm metallic iron absorber. Note that in the Mössbauer spectra of ^{119}Sn, 1 mm/s is equivalent to the energy of 8.0×10^{-8} eV. All spectra were analyzed by least-squares fitting of the Lorentzian-shape absorption lines or quadrupole-split doublets. The final parameters of the fits, including isomer shift (IS), quadrupole splitting

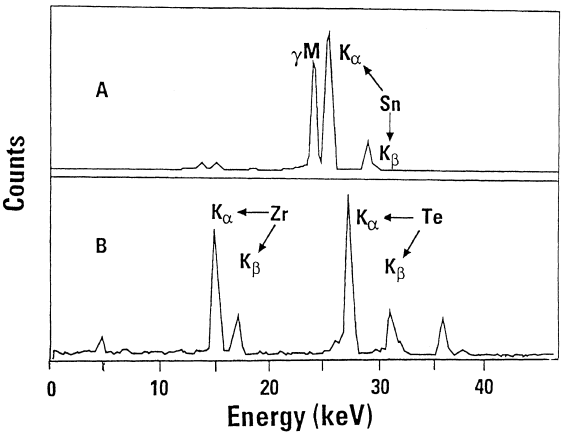

Fig. 1. Spectra of γ- and X-rays recorded with 1×2cm^2 intrinsic planar Ge detector. (a) emission spectrum of the $Cs^{119}SnO_3$ Mössbauer source. (b) spectrum of Zircaloy-4 from a pressure tube after 25 years of service in a power reactor (~18 full-power years); the spectrum was obtained 9 years after extraction of the tube from the reactor. The different peaks are identified as 15.7 and 17.7 keV – Zr K_α and K_β X-rays; 23.9 keV – ^{119}Sn Mössbauer γ-rays; 25.2 and 28.5 keV – Sn K_α and K_β X-rays, 27.4 and 31.0 keV – Te K_α and K_β X-rays.

(QS), width of individual lines (W), and the total and relative areas (A_t and A_r) of spectral components, are listed in Tables 1–3.

The Zircaloy-2 and Zircaloy-4, having typical commercially available compositions, were obtained from Teledyne Wah Chang, Albany. Binary Zr–Sn alloys, with tin concentrations of 0.1%, 1.1% and 8.0%, were prepared by arc melting under argon. The specimen of 0.1% Sn–Zr was enriched in 95% ^{119}Sn and was obtained in single-crystal form. All other specimens has natural isotopic composition. Zircaloys and all Zr–Sn alloys under study had a single-phase α-Zr structure. Two experimental alloys, with the compositions Zr–1Nb–1Sn–0.4Fe (Zirlo) and Zr–3.5Sn–1Nb–1Mo–0.1Fe (Excel) were also examined. These alloys have a two-phase structure, with the α-phase containing Sn, and the Nb-rich β-phase containing Fe and Mo.

According to the phase diagram of the Zr–Sn system [5,6], the solid solution of Sn in α-Zr is metastable and the Zr_4Sn phase may precipitate by aging at a moderate temperature. The Mössbauer parameters of this phase were not known. The specimen of Zr_4Sn was fabricated by a multistage process of heating at 1200°C and grinding. Because Zr_4Sn is very oxygen-sensitive at high temperatures (decomposes at 3 at.% O_2 above 1050°C [14]), the fusion was performed under vacuum.

The Mössbauer absorbers were prepared by diamond-saw cuts from larger pieces of stock materials, in the form of 0.1–1 cm^2 platelets, usually ranging in thickness from 60 to 100 μm, although the specimens as thick as 200 μm were also measurable. To find the op-

timum absorber thickness experimentally, Mössbauer spectra of a series Zircaloy absorbers with different thicknesses were taken. The statistical quality (signal-to-noise) of Mössbauer spectrum is defined as $S/N = Z_\infty(\varepsilon/2)^{1/2}$, where Z_∞ is count rate beyond resonance, and ε is the magnitude of the resonant effect. The dependence of S/N on the absorber thickness is presented in Fig. 2, together with count rate and experimental resonant effect data. This figure shows that the experimentally determined signal-to-noise ratio as a function of the Zircaloy absorber thickness has a broad maximum for absorbers $\sim$ 50–100 μm thick. The theoretically predicted optimum absorber thickness $t = 2/\mu_e$ [15], where μ_e the electronic mass absorption coefficient, is $\sim$70 μm, in good agreement with the experimental data.

In addition, we examined the specimens of Zircaloys, Excel and Zirlo, which were irradiated in a heavy-water research reactor (NRU) at the Chalk River Laboratories (CRL) and in a fast-breeder reactor (EBR-2) at Idaho Falls. The specimens of Zircaloys, which were retrieved from the core of pressurized heavy-water (CANDU) reactors after many years of service in Rolphton (NPD) and Pickering (Unit 2) nuclear generating stations, were also examined. The irradiation conditions of these specimens will be described in Section 3.4. Mössbauer spectra of irradiated specimens were obtained several years after extraction from the reactors.

Because of the neutron capture, the abundance of ^{119}Sn decreases as a function of neutron fluency as follows:

$$^{119}\mathrm{Sn}(t) = [^{119}\mathrm{Sn}(0) + ^{118}\mathrm{Sn}(0)(1 - \exp(-\sigma^{118}\gamma\Phi t))]\exp(-\sigma^{119}\gamma\Phi t), \quad (1)$$

where ^{118}Sn(0) and ^{119}Sn(0) stand for initial isotopic abundances (24.2 and 8.6% respectively), t is time, Φ is the thermal-neutron flux, and $\sigma^{118}\gamma = 4$ mb and $\sigma^{119}\gamma = 2$b are corresponding thermal-neutron capture cross sections. The abundance of ^{119}Sn calculated according to Eq. (1) as a function of time in the thermal neutron flux of 5×10^{18} n/m^2 s is shown in Fig. 3. As seen after twenty years the ^{119}Sn abundance would decrease to about half of its original natural value.

3. Results of measurements

3.1. Reference specimens

As seen in Fig. 4, the ^{119}Sn Mössbauer spectra of reference tin alloys and oxides of interest differ considerably. The obtained parameters of the reference spectra are collected in Table 1. The value of IS and QS of the resonant absorption lines can be used to identify the chemical environment of tin atoms. The corresponding IS–QS diagram is shown in Fig. 5.

The spectrum of usual metallic tin in β-Sn (white) phase represents a broad absorption line with the isomer shift IS = 2.49 mm/s and quadrupole splitting QS = 0.43 mm/s; the latter is ascribed to a tetragonal unit cell symmetry of β-Sn. Tin additives in α-Zr in a range of 0.1–8% yield IS = 1.69 to 1.74 mm/s. The

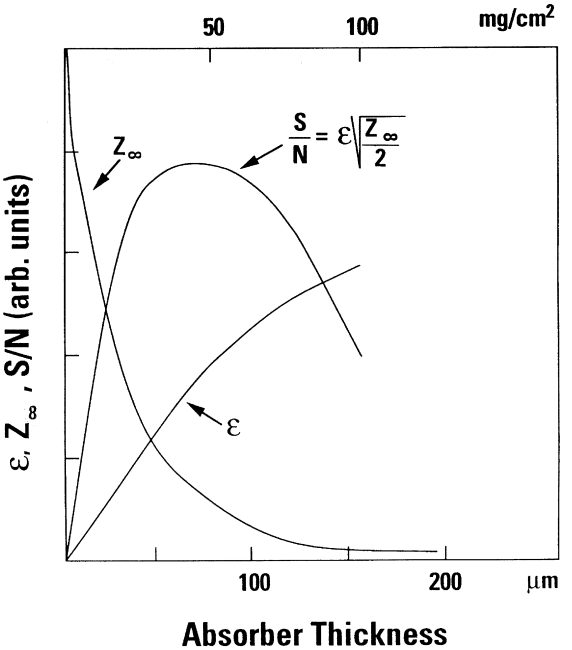

Fig. 2. The magnitude of the resonant effect, ε, in ^{119}Sn Mössbauer transmission spectra of Zircaloy-2 and -4 plotted as a function of the absorber thickness, (B) the dependence of the count rate, Z_∞, for 23.9 keV γ-rays in zirconium on the absorber thickness, and (C) calculated signal-to-noise ratio, $S/N = Z_\infty(\varepsilon/2)^{1/2}$, as a function of absorber thickness.

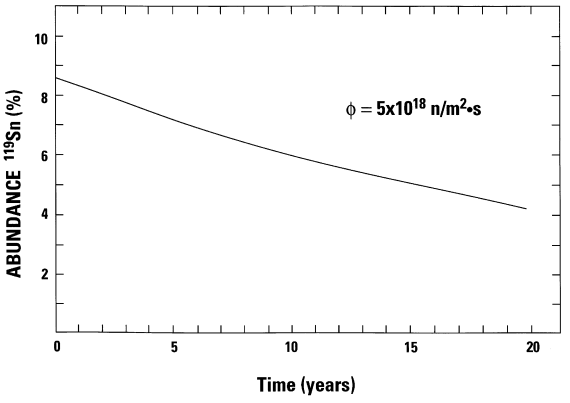

Fig. 3. The depletion of ^{119}Sn as a function of thermal neutron flux-years.

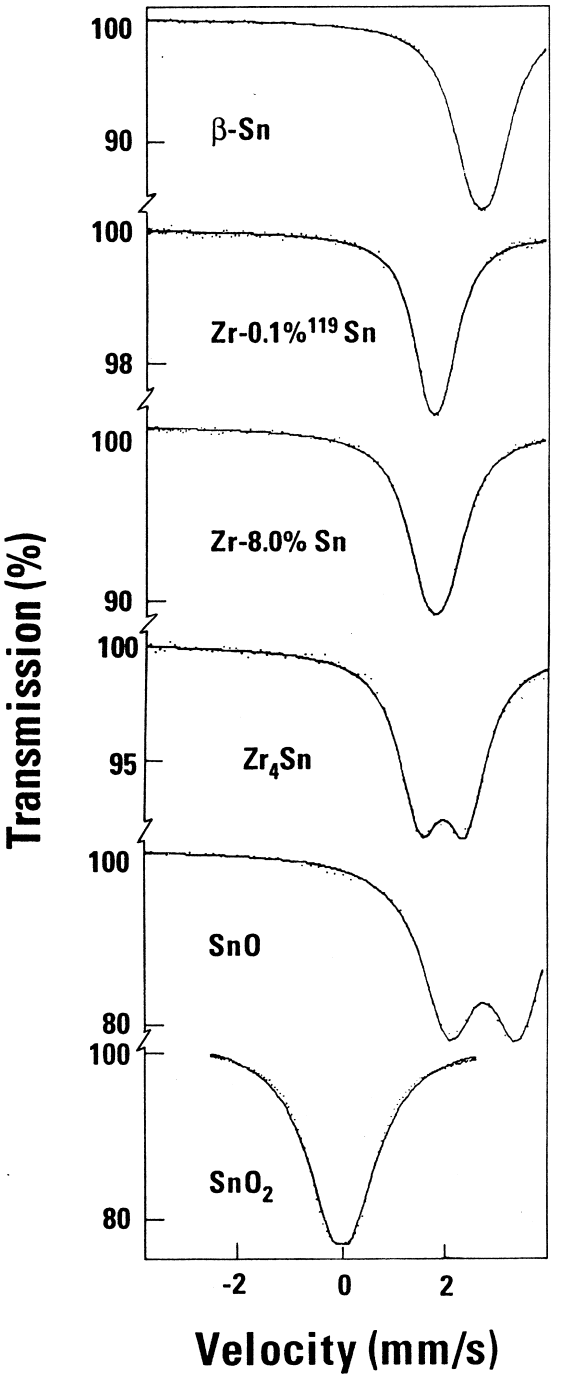

Fig. 4. Mössbauer spectra of 23.9 keV γ-rays of ^{119}Sn in reference specimens of β-Sn, Zr–0.1%Sn, Zr–8%Sn, Zr_4Sn, SnO and SnO_2.

smaller value of the isomer shift than in β-Sn indicates that the electron density at Sn nuclei in α-Zr is smaller than that in β-Sn. The measured IS values are in good agreement both with experimental [16] and theoretical [17] data for Sn located on substitutional sites in α-Zr. The quadrupole splitting, QS = 0.35 to 0.45 mm/s, is caused by the electric field gradient ascribed to hexagonal unit cell symmetry of α-Zr. As Table 1 shows, the magnitude of IS is virtually the same in low-tin (Zr–0.1% Sn) alloy as in high-tin (Zr–8% Sn) alloy.

In low-tin alloys (0.1 and 1% Sn), the experimental linewidth, W = 0.75 to 0.79 mm/s, was only slightly greater than the natural linewidth, $2\Gamma = 0.65$ mm/s. Significantly greater linewidth, $W = 0.95$ mm/s, was observed in Zr–8% Sn specimen. This apparent line broadening can be ascribed to the presence of Zr_4Sn precipitates. The Zr_4Sn has a tetragonal crystal structure (space group *Pm3n*), capable of generating larger electric field gradient at Sn nuclei than in the case of solid solution Sn in α-Zr. As seen in Fig. 4, the reference Zr_4Sn compound shows a distinct isomer shift (IS = 1.81 mm/s) and a fairly large electric quadrupole splitting (QS = 0.86 mm/s).

Fig. 4 also shows, for comparison, the Mössbauer spectra of stannous and stannic oxides (SnO and SnO_2 respectively). The spectra of these oxides were obtained using 50 mg/cm^2 absorbers. The spectra of SnO and SnO_2 are distinctly different from the spectra of β-Sn, Sn dissolved in α-Zr, as well as Zr_4Sn. The obtained IS and QS values for SnO and SnO_2 are in good agreement with the tabulated reference data [19]. Large differences between IS and QS parameters of both oxides reflect the fact that Sn(II) ion has a $4d^{10}5s^2$ configuration, and Sn(IV) ion has $4d^{10}$ electronic configuration. As a result, the s-electron density at tin nuclei, and therefore the IS value, is smaller in SnO_2 than in SnO. The presence of large QS in SnO is ascribed to 5sp hybridization in Sn(II), whereas the lack of QS in SnO_2 is related to spherical symmetry of Sn(IV) ion.

3.2. Unirradiated Zircaloy-2, Zircaloy-4, Excel and Zirlo

The ^{119}Sn Mössbauer spectra of unirradiated specimens of Zircaloy-2, Zircaloy-4, Excel and Zirlo are compared in Fig. 6. The spectra of all these alloys are practically identical. The parameters of these spectra are given in Table 2. Determined from the measurements mean value of the isomer shift, IS = 1.68 mm/s, and quadrupole splitting, QS = 0.36 mm/s, coincide with the IS and QS values found in 0.1 and 1% Sn–Zr alloys (cf. Table 1). The measured IS and QS are consistent with Zircaloy-2 values, IS = 1.5 mm/s and QS = 0.38 mm/s, reported by Barb et al. [20]. The latter results could be quite imprecise given the low statistical quality of the spectra recorded at that time.

The lack in the spectra of the signal other than Sn in α-Zr solution is in agreement with the studies of Igrushin et al. [21] and Chekin et al. [22], who thoroughly investigated the formation of phases precipitated in zirconium-based ternary alloys Zr–M–Fe, where M = Sn,

Table 1
Results of the ^{119}Sn Mössbauer spectroscopic analyses of reference specimens. IS is the isomer shift with respect to ^{119}Sn in a $Ca^{119m}SnO_3$ source, QS is the electric quadrupole splitting, W is the full linewidth at half maximum, A_t and A_r is the total and relative spectral area, respectively. Last digit(s) errors are given in parentheses

Specimen	IS (mm/s)	QS (mm/s)	W (mm/s)	A_t (arb. u.)
β-Sn (white, tetr.)	2.49 (1)	0.43 (1)	0.94 (1)	0.247
Zr–0.1%^{119}Sn	1.69 (1)	0.33 (1)	0.75 (2)	0.026
Zr–1%Sn	1.74 (1)	0.43 (3)	0.79 (6)	0.018
Zr–8%Sn	1.72 (1)	0.41 (1)	0.95 (1)	0.131
Zr_4Sn	1.81 (1)	0.86 (1)	0.97 (2)	0.129
SnO	2.67 (1)	1.34 (1)	1.25 (1)	0.490
SnO_2	−0.02 (1)	0.57 (1)	1.041 (1)	0.328

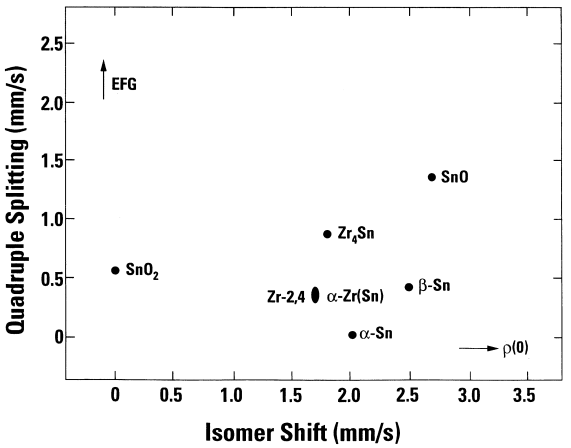

Fig. 5. A correlation between the isomer shifts and quadrupole splittings for tin oxides and Zr–Sn system. The arrows indicate the direction of the growth of the magnitude of the electric field gradient (EFG) and the density of electrons ($\rho(0)$) at the sites of ^{119}Sn nuclei.

V, Cr, Nb, Mo and Ta (∼0.5%, 1% and 2.5%) and which contained Fe (∼0.2% to 0.3%). By measuring Mössbauer spectra they investigated the influence of various alloying elements on the local neighborhood of Fe impurity atoms. With the exception of Zr–Sn–Fe, in all other systems prominent ternary precipitates have been observed.

3.3. Oxygenated alloys

The specimens of Zircaloy-4 were oxidized in air at several temperatures between 500°C and 1200°C. As the second to the top spectrum in Fig. 7 indicates, oxidation at 500°C for 16 h resulted in no apparent change in the Sn, but after oxidation at 600°C for 2 d, a considerable amount of Sn (∼50%) in a form of SnO_2 (quadrivalent Sn(IV)), represented by a doublet near 0 mm/s, had formed. After oxidations in air at 700°C (1 d), 1000°C (2 h) and 1200°C (1 h), all Sn was oxidized to the SnO_2,

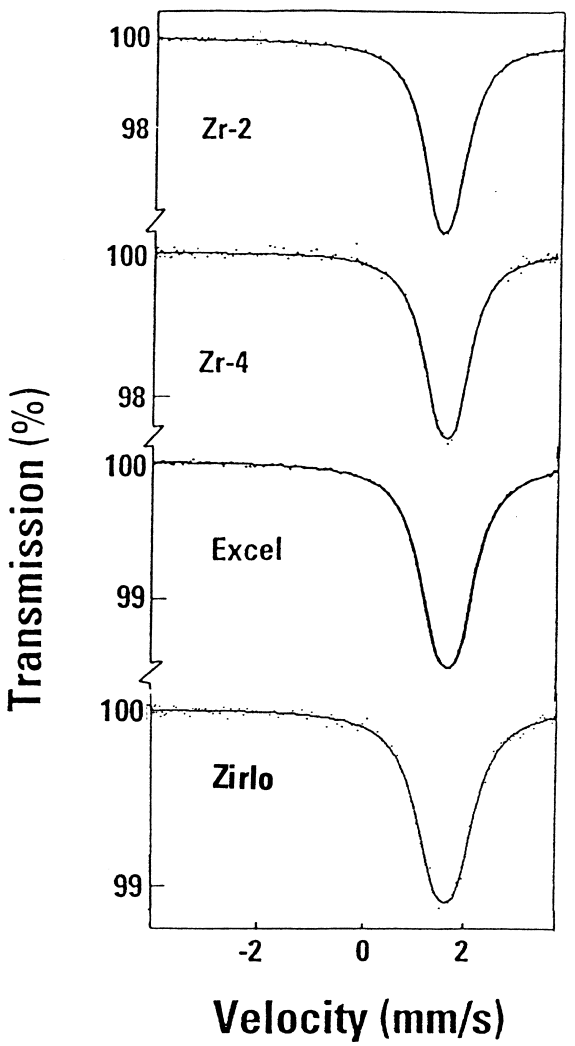

Fig. 6. Mössbauer spectra of 23.9 keV γ-rays of ^{119}Sn in unirradiated Zircaloy-2, Zircaloy-4, Excel and Zirlo.

and no features attributable to SnO or metallic tin were present. The spectral parameters of oxidized Zircaloys are given in Table 3.

Table 2
Results of the ^{119}Sn Mössbauer spectroscopic analyses of unirradiated Zircaloy-2, Zircaloy-4, Excel and Zirlo

Specimen	IS (mm/s)	QS (mm/s)	W (mm/s)	A_t (arb. u.)
Zircaloy-2	1.66 (1)	0.32 (1)	0.74 (1)	0.032
	1.69 (1)	0.40 (1)	0.85 (2)	0.028
	1.70 (1)	0.40 (1)	0.81 (2)	0.028
Zircaloy-4	1.71 (4)	0.34 (1)	0.76 (2)	0.022
	1.70 (1)	0.40 (2)	0.97 (4)	0.030
	1.71 (1)	0.52 (3)	0.81 (6)	0.033
1000°C/vac/40 h	1.60 (1)	0.38 (1)	0.86 (2)	0.025
Excel	1.71 (1)	0.39 (1)	0.80 (1)	0.078
Zirlo	1.67 (1)	0.47 (2)	0.74 (3)	0.020

These results can be compared with the results of Chekin et al. [22] and Babikova et al. [23,24] who investigated the redistribution of tin atoms in Zr–1% Sn during corrosion in water and steam at 350°C. By combining Mössbauer spectroscopy with a chemical stripping method, they observed, in addition to SnO_2, significant fractions of tin in a form of SnO and β-Sn. These two latter phases were not observed in our measurements. However, information derived from corrosion products stripped from the surface by chemical methods must be taken with caution because the stripping process may significantly alter the corrosion products.

^{119}Sn Mössbauer spectra of oxidized Zircaloy-4 were also taken on chemically stripped oxides. The final valent form of tin (Sn(IV)) did not differ in Zircaloys-4 with low and high content of tin. It was however notably affected by high concentration of LiOH in oxidizing solution, which resulted in production of a small spectral component (<14% of spectral area) ascribed to poorly defined Sn(I) species. This can be ascribed to the fact that due to very low solubility of Sn in ZrO_2 (baddeleyite), Sn is partly expelled on oxidation from the bulk to the surface, and therefore can assume lower oxidation state in less reducing LiOH environment.

When Zircaloy-2 was exposed to a limited quantity of oxygen at a temperature of 1900°C, a solid Zr–Sn–oxygen solution was formed. The results of this experiment were discussed in detail elsewhere [25]. For both concentrations of oxygen studied, 11.8 at.% O_2 and 26.1 at.% O_2, the Mössbauer parameters of the Zr–Sn–oxygen solid solution phase remained in the range observed for Zr–Sn solid solution (see Table 3, bottom). This is consistent with the fact that Sn is a strong reducing agent in Zr, and that Zircaloy, like zirconium, can accommodate atomic oxygen up to ~ 30 at.%, from room temperature to the solidus of the mixture. At higher oxygen concentrations, phase separation occurs and a hyperstoichiometric Zr_2O_x phase appears.

3.4. Reactor-irradiated specimens

Fig. 8 shows the Mössbauer spectra of several reactor-irradiated specimens; the corresponding spectral parameters are given in Table 4. The first three spectra from the top were obtained for specimens that had been irradiated in a fast-breeder reactor EBR-2 at Idaho Falls, in a fast neutron flux of 9.7×10^{17} n/m^{2}s ($E > 1$MeV). Specimens of Zircaloy-2 were in the form of a 3 mm-sized 0.12 thick discs. One of them was irradiated at 55°C to fluence of 2.4×10^{24} n/m^2 and another was irradiated at 320°C to a fluency of 7.4×10^{24} n/m^2 [2]. The specimen of Excel was irradiated at 390°C to a fluence of 16.2×10^{25}n/m^2; the dimensions of this specimen were $12 \times 4 \times 0.11$mm. Exactly similar spectrum was also observed for specimen of Zirlo, which was irradiated at 300°C to fluence of 7.5×10^{24}n/m^2 in a heavy-water research reactor (NRU) at Chalk River.

Similar to specimens of Excel, Zirlo and Zircaloy-2 irradiated in test reactors, a spectrum of Zircaloy-4 irradiated in power reactor indicated only Sn in α-Zr. The latter specimen was extracted from the central section of one of the pressure tubes in the pressurized heavy-water Nuclear Power Demonstration (NPD) reactor in Rolphton, Ontario, after its decommissioning in 1987 [26]. This 20 MW(e) prototype CANDU reactor was in service for 25 years (~ 18 full-power years). The 4 m long × 83 mm diameter tube operated under a pressure of 86 MPa and an outlet water temperature of ~ 275°C. The alloy was subjected to fast-neutron flux of 1×10^{17}n/m^2 s; the accumulated fluence of 5.6×10^{25}n/m^2 was equivalent to ~ 8–11 displacements per atom. The specimen measured $4 \times 9 \times 0.17$ mm and, as a result of neutron irradiation, was significantly depleted in ^{119}Sn.

The spectrum of a Zircaloy-2 oxide scrape, third from the bottom in Fig. 8, differs from all other spectra of irradiated specimens. The scrape had been extracted from the high-flux/high-temperature area of a fuel channel from one of the Pickering CANDU reactors (Unit 2) after about 10 years of service. The specimen

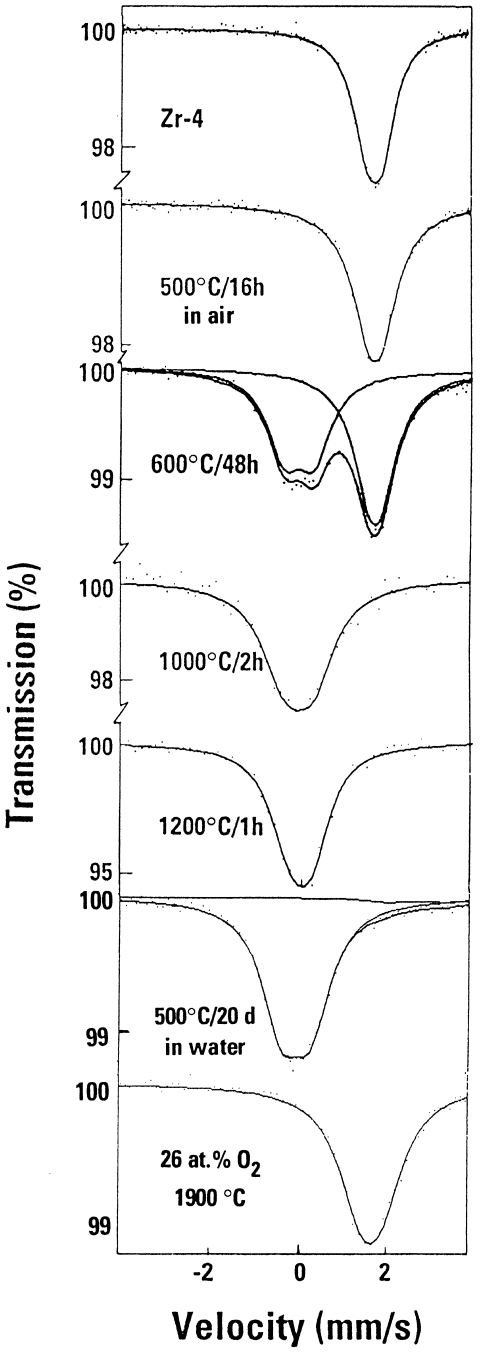

Fig. 7. Mössbauer spectra of 23.9 keV γ-rays of ^{119}Sn in unirradiated Zircaloy-4 oxidized at various temperatures and oxygen pressures

was obtained by scraping an inner (fuel and water-exposed) face of a pressure tube during a routine in-core inspection. The size of the specimen was $3 \times 4 \times 0.15$ mm, with about 40 μm being the oxide phase and the rest being the base alloy. 78% of the spectral area can be ascribed to Sn in solid solution in α-Zr (the base alloy substrate) and 22% to Sn(IV) in SnO_2 presumably formed in the oxide film on the surface of the scrape.

Another application of ^{119}Sn Mössbauer spectroscopy in nuclear reactor issues is demonstrated by the spectrum displayed at the bottom of Fig. 8. In this case, we have examined the chemical form of tin in filterable deposits extracted from the primary coolant of one of CANDU reactors at Darlington nuclear power station. The deposits were collected by passing heavy water from the reactor through a 0.45 μm pore-sized, 47 mm diameter Millipore membrane. The collected particulates contained mostly iron oxides, with miniscule quantity of zirconium and tin-bearing particulates. The Mössbauer emission spectrum of radioactive ^{119}Sn in filter deposits was obtained using a SnO_2 absorber. The obtained spectrum shows that tin in these particulates occurs in a form of Sn(IV), probably as SnO_2 (from mechanical wear and corrosion of Zircaloy-4 fuel cladding). This form of tin was identified earlier in Mössbauer spectra of oxidized Zircaloy-2 scrapes extracted from a fuel channel of Pickering reactor.

4. Discussion

Before discussing the obtained results in more detail it is worthwhile to recall some information regarding the relationship between the IS and QS in Mössbauer spectra of ^{119}Sn. As is well known, the isomer shift is proportional to the density of electrons $\rho(0)$ on the nuclear positions (the contact density): IS $\sim \rho(0) - \rho_{\mathrm{ref}}(0)$, where $\rho_{\mathrm{ref}}(0)$ is the electron density at tin nuclei in reference compound (here $CaSnO_3$). In the case of ^{119}Sn, the greater IS value indicates a larger electron density at the nucleus. The value of IS is highly sensitive to the changes of the configuration of the atom's valence electrons. The QS is determined by the tensor of the electric field gradient (EFG) at the tin nuclei, which reflects both the symmetry and covalency of the electron shells and the symmetry of the crystal sites occupied by tin atoms. The magnitude of the QS is proportional to the quantity $V_{zz}(1 + \eta^2/3)^{1/2}$, where V_{zz} is the principal component and $\eta = V_{xx} - V_{yy}/V_{zz}$ is the asymmetry parameter of the 3×3 EFG tensor.

By measuring the IS and QS of a metallic or oxidized system it is possible to investigate the electron-density distribution changes that reflect the features of the interaction between atoms when an alloy, intermetallic compound or oxide is formed. As Fig. 5 shows, the points in IS–QS coordinates can provide a unique signature of different tin species of interest here, thus allowing their identification in the examined material.

The systematics of ^{119}Sn isomer shifts in various metals [16,17] show that the range of isomer shift for tin in most metallic environments is relatively narrow, from

Table 3
Results of the ^{119}Sn Mössbauer spectroscopic analyses of oxygenated Zr–8% Sn and Zircaloy-4 specimens

Specimen	IS (mm/s)	QS (mm/s)	W (mm/s)	A_t (arb. u.)	A_r (%)
Zr–8% Sn 550°C/16 h	1.68 (1)	0.34 (2)	0.94 (3)	0.020	95.5
	2.50	0.43	0.94		4.5
Zr-4 500°C/16 h	1.73 (1)	0.34 (4)	1.03 (6)	0.015	100
500° C/21 d Chemically stripped	0.05 (1)	0.63 (1)	1.03 (3)	0.011	95
	2.8 (2)	1.6 (3)	1.2		5
600°C/2 d	1.67 (1)	0.26 (3)	0.89 (2)	0.028	53
	0.02 (1)	0.65 (1)	0.88 (1)		47
700°C/1 d	0.05 (1)	0.63 (2)	0.99 (5)	0.012	100
1000°C/2 h	−0.00 (2)	0.66 (5)	1.13 (9)	0.037	100
1200°C/1 h	0.01 (1)	0.48 (3)	1.04 (5)	0.068	100
Corroded with LiOH	0.04 (1)	0.48 (1)	0.91 (2)	0.022	86
	2.4 (1)	2.1 (1)	2.0 (2)		14
Zr-4/11.8 at.% O_2 – heated at 1900°C	1.71 (1)	0.49 (2)	1.13 (5)	0.027	100
26.1 at.% O_2 – heated at 1900°C	1.70 (1)	0.45 (2)	1.22 (4)	0.012	100

about 1.1–3.2 mm/s. A linear correlation between IS and the Miedema scale electronegativity ϕ_M of the matrix was obtained for Sn admixtures in pure metals. The following relations were found [16] between IS and $\Delta\phi = \phi_M - \phi_{Sn}$:

$$\text{IS (mm/s)} = 2.59 - 1.74\Delta\phi \quad \text{for non-transition metals,} \tag{2a}$$

$$\text{and} \quad \text{IS (mm/s)} = 1.7 - 0.2\Delta\phi \quad \text{for transition metals.} \tag{2b}$$

The drastic weakening of the dependence of IS on ϕ_M for transition metals as compared to non-transition metal matrices has been ascribed to the decrease of the s-electron component of the wave function of a tin atom as a result of sd electron hybridization. Fig. 9 presents the lines drawn according to the formulas given above. For tin in zirconium, $\phi_{Sn} = 4.15$ V and $\phi_{Zr} = 3.45$ V [18], the relationship (2b) gives IS = 1.84 mm/s, which is fairly close to our average experimental value for Sn in Zr, IS = 1.70 (1) mm/s, and with the data given in Ref. [16], IS = 1.72 (2) mm/s.

Measuring the spectra of specimens retrieved from nuclear power reactors took much longer (5 to 10 times) counting time than for unirradiated samples. A comparison of the spectral areas of the irradiated absorbers (Table 4) with the data for unirradiated absorbers shows that the resonant absorption area for Zircaloy-2 from the Pickering reactor and Zircaloy-4 from the NPD reactor was significantly lower than for unirradiated specimens of comparable thickness. According to Eq. (1) and Fig. 3, this is ascribed mostly to the fact that the resonant ^{119}Sn isotope becomes depleted by a thermal neutron $^{119}\text{Sn}(n,\gamma)$ capture reaction with a high cross section, as compared with a low cross section of $^{118}\text{Sn}, (n,\gamma)^{119}\text{Sn}$ reaction. Depletion of the ^{119}Sn isotope was less pronounced after irradiations in a fast-breeder reactor, because of a considerably lower thermal -neutron flux (<10 times).

Electron microscopic observations of particles of Sn, ZrSn and Zr_4Sn, as well as various SnNi compounds in Zircaloy-2 and Sn precipitates in Zircaloy-4, were reported by Kuwae and co-workers [8], and by some other researchers. These Sn-based precipitates were found mainly in β-phase-quenched materials. However, because β-quench is an uncommon heat treatment for these alloys, there is very little corroborating evidence in the literature to support these observations. In later studies, it was also recognized that Sn precipitates in Zircaloys can be an artifact caused by the redeposition of dissolved Sn during TEM sample preparation [9]. In the present work we did not observe any spectral features that could be clearly ascribed to such intermetallics. It is to be noted that intermetallic Sn–Fe phases have not been seen as well by Igrushin et al. [21], who investigated additions of Sn, V, Cr, Mo, Nb and Ta on the local neighborhood of Fe impurity atoms in α-Zr.

In the case of neutron-irradiated alloys, Griffiths [1] reported Sn–FeCr precipitates in Excel after irradiation to moderate fluences ($\sim 5 \times 10^{25}$ n/m^2) at about 400°C. He stated that the radiation-enhanced diffusion formed this Sn-containing phase under irradiation in the high-temperature range of 360–435°C. It has also been postulated that the formation of Sn-rich precipitates may also affect corrosion by reducing the Sn supersaturation in the Zr matrix [2]. Although the Sn-rich precipitates were expected to form at these temperatures, they could not be detected in the limits of the Mössbauer measurements resolution, as explained below.

Because of small variation of the isomer shift of Sn in transition metal hosts, the Sn–FeCr precipitate – even if present in the alloy – might not be distinguished in the Mössbauer spectra. According to Eq. (2b) (cf. also Fig. 9), and in agreement with the experimental data of

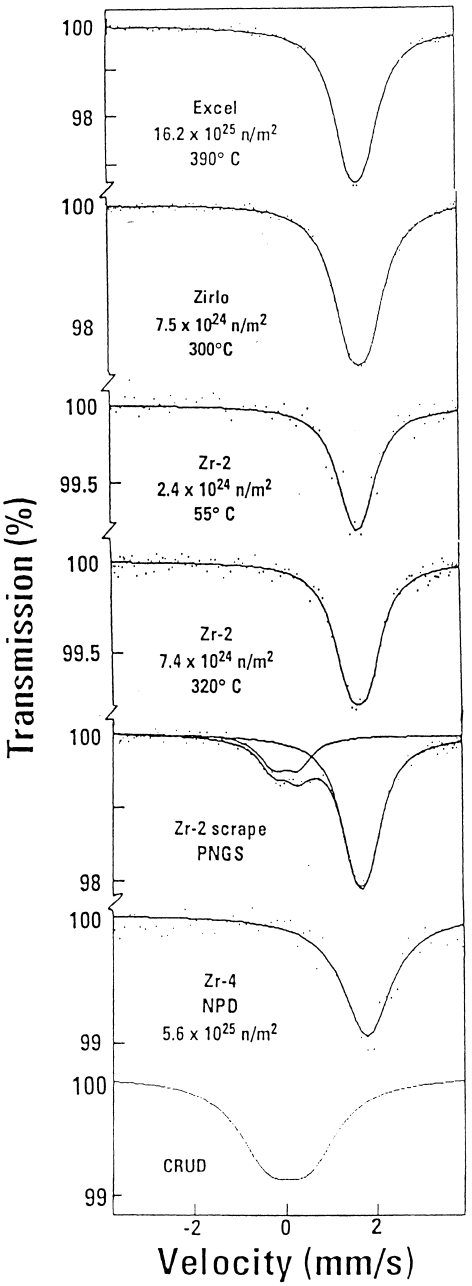

Fig. 8. Mössbauer spectra of 23.9 keV γ-rays of ^{119}Sn in neutron-irradiated specimens of Excel, Zircaloy-2, Zircaloy-4, as well as Zircaloy-2 oxide scrape removed from the pressure tubes and filtered deposits from primary heavy water coolant of CANDU reactors.

Delyagin and Nesterov [16], for Sn totally surrounded by Fe and Cr, the expected isomer shift should be $IS = 1.58 \pm 0.02$ mm/s. Thus, the superposition of a small peak due to Sn–FeCr could result in some distortion of the absorption line of Sn in α-Zr, but this has not been clearly identified in measured spectra.

The observation of SnO_2 in the oxide scrape extracted from the Zircaloy-2 pressure tube was not expected on the basis of thermodynamic consideration, and therefore is interesting and can be quite consequential. As was pointed in Section 3.2, in the laboratory, the formation of the SnO_2 was seen only in the specimens of Zircaloy, air-oxidized at 500°C and at higher temperatures. As a rule of the thumb, one should not expect to see any SnO_2 until all zirconium is oxidized. Further, because the solubility of tin is reduced in oxygenated zirconium, it was rather expected that a segregated tin-rich layer would be formed on the surface when the alloy was heated. Apparently, the oxidation conditions at reactor operating temperatures (~300°C) and at high neutron fluxes ($\sim 10^{18}$/cm^2 s) are quite different from laboratory conditions. Long exposures to radiation at thermal and chemical conditions of the reactor seem to favor formation of SnO_2.

Further applications of ^{119}Sn Mössbauer spectroscopy of Zircaloys would require precise data on the recoilless absorption fractions, f_a, of tin in different relevant phases. The relative areas of the corresponding spectral components, $A_r \sim f_a C$, are proportional to f_a factors and concentrations, C, of different Sn species. In particular, Chekin [22] gives at 300 K, $f = 0.42 \pm 0.04$ for metallic Zr(Sn) phase, $f = 0.38 \pm 0.04$ for Zr(Sn)O_2 oxidized phase, compared with $f = 0.45 \pm 0.02$ for SnO_2. For comparison, the recoilless fraction of β-Sn is quite small at 300 K, $f = 0.04$, as compared with $f = 0.45$ at 78 K and $f = 0.72$ at 4.2 K. The possibility of observation of β-Sn, and possibly some other phases with low f-factors, would be greatly improved performing measurements at low temperatures.

5. Conclusions

Mössbauer spectroscopy of the 23.9 keV γ-rays in ^{119}Sn was used to study the state of tin in α-Zr, and in unirradiated and neutron-irradiated samples of Zircaloy-2 and -4. It proved to be an effective means of looking for tin oxidation state and segregation in these alloys. The spectra of Zircaloys and spectra of Zr–Sn alloys in the composition range 0.1–8% Sn indicated only one quadrupole doublet that is characteristic of the tin in substitutional solid solution with α-Zr, and with no metallic β-Sn. Reactor-irradiated Zircaloys indicated depletion of the resonant ^{119}Sn isotope, but the chemical state of the tin remained unchanged. The Zircaloy-2 oxide scrape extracted from the core of CANDU reactor, and therefore exposed to less than 300°C, showed a SnO_2 component, which in air-oxidized specimens could be observed only at temperatures higher than 500°C.

Table 4
Results of the ^{119}Sn Mössbauer spectroscopy analyses of neutron-irradiated Excel, Zirlo, Zircaloy-2 and Zircaloy-4, as well as of trace quantities of tin in wear particles from primary coolant of a reactor

Specimen	IS(mm/s)	QS(mm/s)	W(mm/s)	A_t(arb. u.)	A_r(%)
Excel irr. 390°C, 16.2×10^{25} n/m^2	1.72 (1)	0.39 (1)	0.89 (1)	0.033	100
Zirlo irr. 300°C, 7.5×10^{24} n/m^2	1.69 (1)	0.44 (1)	0.89 (2)	0.027	100
Zr–2 irr. 55°C, 2.4×10^{24} n/m^2	1.67 (3)	0.25 (10)	0.84 (15)	0.005	100
Zr–2 irr. 320°C, 7.4×10^{24} n/m^2	1.64 (1)	0.43 (2)	0.84 (4)	0.006	100
Zr-2 irr. 290°C, partly oxidized scrape	1.64 (1)	0.32 (2)	0.82 (3)	0.022	78
	−0.02 (3)	0.54 (4)	0.74 (6)		22
Zr-4, irr. 275°C, 5.6×10^{25} n/m^2	1.71 (3)	0.40 (8)	1.0 fixed	0.010	100
Primary coolant crud (emission spectrum)	0.00 (1)	0.88 (14)	0.58 (31)	0.022	100

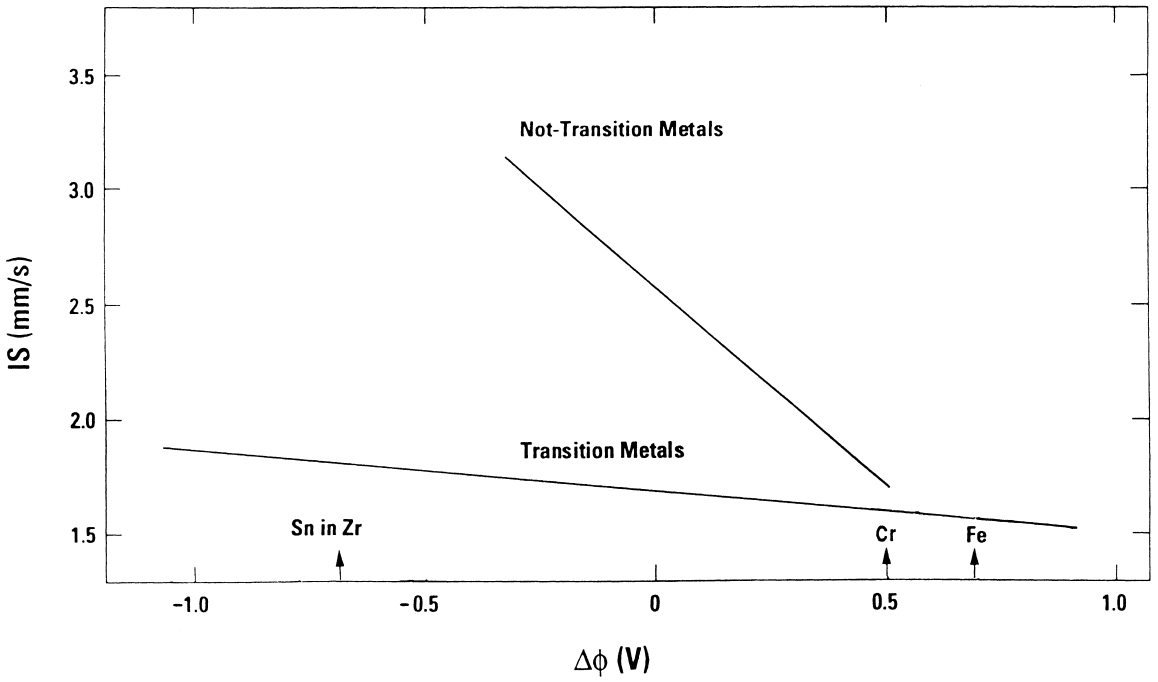

Fig. 9. Isomer shift for ^{119}Sn impurity in transition and non-transition metals vs the relative electronegativity of the matrix $\Delta\Phi = \Phi_M - \Phi_{Sn}$. Adopted from Delyagin and Nesterov [16].

Acknowledgements

The author thanks M. Griffiths and J. McFarlane of AECL, R.B. Adamson of GE Nuclear Energy and B. Cox of the University of Toronto for providing some of the specimens and for helpful discussions.

References

[1] M. Griffiths, R.W. Gilbert, G.J.C. Carpenter, J. Nucl. Mater. 150 (1987) 53.
[2] M. Griffiths, J. Nucl. Mater. 159 (1988) 190.
[3] J.A. Sawicki, J. Nucl. Mater. 228 (1996) 238.
[4] J.A. Sawicki, in: I.M. Robertson, S.J. Zinkle, L.E. Rehn, W.J. Phythian (Eds.), Microstructure of Irradiated Materials, vol. 373, MRS Fall Meeting Symposium Proceedings, Materials Research Society, Pittsburgh, PA, 1994, p. 215.
[5] J.P. Abriata, J.C. Bolcich, D. Arias, Bull. Alloy Phase Diagrams 4 (2) (1983) 147.
[6] D. Arias, L. Roberti, J. Nucl. Mater. 118 (1983) 143.
[7] G.J.C. Carpenter, E.F. Ibrahim, J.F. Watters, J. Nucl. Mater. 102 (1981) 280.
[8] R. Kuwae, D. Sato, E. Higashinakagawa, J. Kawashima, S. Nakamura, J. Nucl. Mater. 119 (1983) 229.
[9] W.J.S. Yang, R.P. Tucker, B. Cheng, R.B. Adamson, J. Nucl. Mater. 138 (1986) 185.

[10] T.Y. Yang, G.P. Yu, L.J. Chen, J. Nucl. Mater. 150 (1987) 67.
[11] O.T. Woo, G.J.C. Carpenter, J. Nucl. Mater. 159 (1988) 397.
[12] J.J. Kai, W.I. Huang, H.Y. Cou, J. Nucl. Mater. 170 (1990) 193.
[13] U. Gonser, in: Microscopic Methods in Metals, ed. U. Gonser, Topics in Current Physics, vol. 40, Springer, Berlin, 1986, p. 409.
[14] Y.-U. Kwon, J.D. Corbett, Chem. Mater. 4 (1992) 187.
[15] G.J. Long, T.E. Cranshaw, G. Longworth, Mössbauer Eff. Ref. Data J. 6 (1983) 42.
[16] N.N. Delyagin, V.I. Nesterov, Zh. Eksp. Teor. Fiz. 91 (1986) 2303; Sov. Phys-JETP 64 (1986) 1367.
[17] A. Svane, Phys. Rev. Lett. 60 (1988) 2693.
[18] A.K. Niessen, F.R. de Boer, R. Boom, P.F. de Chatel, W.C.M. Mattens, A.R. Miedema, Calphad 7 (1983) 51.
[19] J.G. Stevens, Hyperf. Interact. 13 (1983) 221.
[20] D. Barb, E. Burzo, S. Constantinescu, L. Diamandescu, A. Marian, D. Tarina, Rev. Roum. Phys. 20 (1975) 103.
[21] V.V. Igrushin, V.G. Kirichenko, I.A. Petel'guzov, V.V. Chekin, Fiz. Met. Metalloved. 55 (1983) 1143 (in Russian); Phys. Met. Metall. 55 (1983) 92.
[22] V.V. Chekin, V.G. Kirichenko, A.I. Velikodnii, A.S. Yatsenko, I.A. Petel'guzov, Fiz. Met. Metalloved. 41 (1976) 782 (in Russian); Phys. Met. Metall. 41 (1976) 91.
[23] Yu.F. Babikova, P.L. Gruzin, A.V. Ivanov, V.P. Filipov, I.I. Shtan', V.A. Khaikovsky, V.N. Abramtsev, Metallurg. Metalloved. Chisty. Metall. 12 (1976) 20.
[24] Yu.F. Babikova, P.L. Gruzin, A.V. Ivanov, V.P. Filipov, Izv. Vyssh. Ucheb. Zaved. Fiz. 1 (1981) 70.
[25] J. McFarlane, J.C. LeBlanc, Tin release from oxygenated Zircaloy-4, Atomic Energy of Canada Limited, Report-11666, February 1997.
[26] C.E. Coleman, B.A. Cheadle, A.R. Causey, P.C.K. Chow, P.H. Davies, M.D. McManus, D.K. Rodgers, S. Sagat, G. Van Drunen, in: LF.P. Swam, C.M. Eucken (Eds.), Zirconium in Nuclear Industry: Eighth International Symposium, ASTM STP 1023, ASTM, Philadelphia, 1989, p. 35.